Multi-Layer Multi-User MIMO with Cylindrical Arrays under 3GPP 3D Channel Model for B5G/6G Networks

Temperature dependence of photoconductivity and noise in CdS-based devices

A. Carbone and P. Mazzetti
INFM, Dipartimento di Fisica del Politecnico di Torino, Corso Duca degli Abruzzi 24, 10129 Torino, Italy
(Received 11 October 1994)

Experimental results concerning photoconductance and noise vs light intensity and wavelength for different values of the temperature in a CdS-based photoconducting device are presented and compared with the prediction of a theory based on a barrier-type photoconduction model developed in a previous paper. Temperature is varied from 300 to 225 K, a range where photoresponsivity, noise, and a few parameters entering the theory present a change of about one order of magnitude. At lower temperatures the occurrence of persistent photoconductivity prevents a suitable check of the model. Relative variations of the responsivity and of the noise with temperature are accounted for by the theory without the introduction of free parameters, while absolute values of these quantities are also correctly reproduced in the whole explored range of light intensity and wavelength, assuming a suitable value for the light quantum efficiency. Other parameters entering the theory were either measured on the device or taken from literature. The analysis of the results also shows that the noise component related to the barrier height spontaneous fluctuations is strongly influenced by temperature changes, while the noise components related to the electron-transport process within the conduction band of CdS are practically unaffected by temperature in the range of variation of this quantity given in this paper.

I. INTRODUCTION

A theory of the photoconductivity and current noise in CdS-based devices, developed on the basis of a barrier-type photoconduction mechanism,[1–3] has been reported in previous papers.[4,5] According to this model, the electrical conductance of the device is related to the height of a light-sensitive potential barrier localized in proximity to the metal electrodes. As quantitatively described in Ref. 4, this barrier exists at the metal-insulator contact even if the contact is, strictly speaking, Ohmic, as it happens in the case of CdS-In contacts. The effect of the light results in a positive trapped charge, related to the ionization of deep donor centers or the creation of immobile holes, which changes the barrier height and thus the current injected within the photoconducting material. As will be extensively described in the following, the variation of this barrier with light correctly accounts for the behavior of the conductance vs light intensity and wavelength.

The barrier model also accounts for the dependence of current noise on light intensity and wavelength. A complete theory of photoconductance noise based on this model has been developed in Ref. 4. The main results of this theory will be summarized in Sec. III. Here we want to point out that, in addition to the usual fluctuation processes related to the charge transport in semiconductors, a further noise component is generated by the barrier height fluctuation. This component, which has been called the photoinduced noise component, is very sensitive to the light wavelength near its critical value λ_{gap}, corresponding to the energy gap of the photoconducting material. Conversely, the intrinsic noise component, related to the transport process within the photoconducting material, shows only a slight increase of the $1/f$ component when $\lambda < \lambda_{gap}$. This may be due to the strong increase of the light absorption and to the corresponding increase of the electrical conduction at the photoconductor surface, where the $1/f$ noise is mainly generated.

An important result of the theory concerns the possibility of evaluating the photoinduced noise component without the introduction of adjustable parameters, using experimental data concerning conductance and relaxation-time measurements as a function of light intensity and wavelength.

An extended check of the theory, using experimental data taken at room temperature, has been given in Ref. 5. In the present paper another check of the theory is made by comparing its results with the experimental ones taken at lower temperatures, where a rather drastic change of several parameters entering the theory takes place. Since the relative changes with temperature of the photoconductance and the photoinduced noise component can be worked out from the theory without the introduction of free parameters, the test of the theory becomes rather stringent. Noise analysis is made under physical conditions where the effect of the photoinduced noise component on the total noise power spectrum is largest. As reported in Ref. 5, at room temperature and at a sufficiently high light intensity, this component is about one order of magnitude larger than the intrinsic component in the low-frequency range. This point will be cleared up in Sec. III, where a summary of the main results of the theory is given.

In Sec. II experimental results taken at different temperatures on a CdS-based device, concerning photoconductance, relaxation, and noise as a function of light intensity and wavelength, are reported. These results are compared with the theoretical predictions in Sec. IV.

II. EXPERIMENTAL RESULTS

All measurements reported in this section were taken on a photoconductor constituted by an Ag-doped CdS

0163-1829/95/51(19)/13261(8)/$06.00

photoconducting film, approximately 1.5×10^{-6} m thick and 2×10^{-2} m wide, with indium Ohmic contacts set about 1 mm apart, and enclosed in an evacuated glass container. The device, already used to obtain the data at room temperature in the previous paper,[5] was fitted within a suitable cryostat with optical windows, which allowed us to change its temperature nearly to that of liquid nitrogen.

Actual temperature measurements of the photoconducting film were made by measuring the power spectrum $\phi(f)$ of the thermal noise of the film in the absence of the bias current and in the presence of light. Even if the specimen was not in thermal equilibrium, the well-known expression $\phi(f)=4kRT$, where R is the photoconductor resistance in the presence of light at the temperature T, and k the Boltzmann constant, was proved to be true theoretically,[6] and was checked experimentally by changing the light intensity and, consequently, the value of R at constant temperature. Comparison with the results obtained at room temperature shows that this method allows to obtain an accuracy of ±2 °C.

The experimental setup used to obtain the reported data has been already described in Ref. 5. Its main aspects are briefly summarized below.

Photoconductance and photoconductance noise measurements as a function of light intensity and wavelength were performed by using a monochromator whose output slit was connected to an optical guide bringing light to the specimen within the cryostat. A beam splitter and a calibrated photocell were used to monitor light intensity. The wavelength resolution of the monochromator was about 3 nm. Noise measurements were performed by means of a digital spectrum analyzer, using a suitable equivalent circuit to perform frequency corrections and to convert voltage fluctuation to photoconductance fluctuation spectra. Details about the equivalent circuit are reported in Ref. 5.

Photocurrent relaxation measurements were performed by superimposing a small rectangular light signal, having a period much longer than the average photocurrent decay time, to the main light source before the input slit of the monochromator. Photocurrent decay pulses, stored in a digital oscilloscope, were analyzed to obtain the average decay time τ_d defined in Sec. III. They were also interpreted as a superposition of exponential decays related to different types of trapping centers. This allowed us to work out the correct shape of the photoconductance noise power spectrum, as described in Sec. III.

It is interesting to note that, particularly at low temperature, the use of a short light pulse instead of the square-wave light signal gives a faster photocurrent relaxation. This is in favor of the interpretation given above of independent recombination processes, since it is expected that longer recombination times are related to centers that require longer excitation times.

The main results concerning photoconductance vs light intensity are reported in Fig. 1 for three values of the temperature, and for light wavelengths slightly above and slightly below the critical wavelength λ_{gap}. Indeed, most of the change of the device responsivity and the photoconductance noise take place in this small range of λ values.

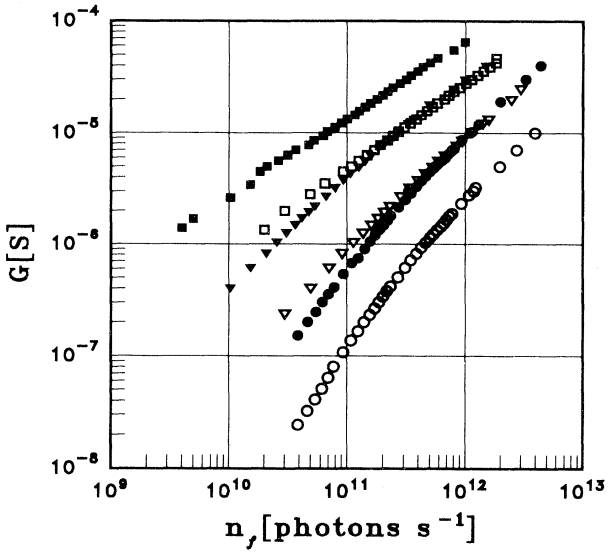

FIG. 1. Electrical conductance G vs photon flux n_f at $\lambda=510$ (filled symbols) and at 490 nm (hollow symbols). The temperature T is equal to 300 (circles), 250 (triangles), and 225 K (squares). The superlinear behavior at room temperature tends to become linear as the temperature is lowered. This is in agreement with the photoconduction model described in Sec. III.

As discussed in Sec. III, where a quantitative interpretation of all the results reported here is given, the observed changes are mostly related to the change of the lifetime of the trapped charge (ionized deep donor centers or trapped holes, depending on the light wavelength), which determine the height of the potential barrier controlling the device photoconductance. A behavior similar to that shown in Fig. 1 is commonly found in the II-VI compounds (Ref. 7 and references therein). The photoinduced noise component, which is related to this barrier height fluctuation, is also affected by the lifetime of the ionized centers, as well as by their time constant distribution. The results reported in Figs. 2 and 3 concern the relative photoconductance fluctuation spectrum taken at two different light wavelengths, slightly above and slightly below λ_{gap}, and related to three different temperatures. It is important to note that the conductance of the device was kept constant in all cases by adjusting the light intensity. In the same figures, theoretical results concerning the photoconductance noise power spectra calculated according to the theory reported in Sec. III are shown.

In order to explain the above results, measurements of other physical quantities in an extended range of light intensities and for different light wavelengths have been performed. The results reported in Fig. 4, concerning the behavior of the average decay time of the photocurrent τ_d vs photoconductance for the two values of λ given above, were obtained from a large set of results of the type reported in Fig. 5, by dividing the area of the relaxation pulse by its maximum height. It should be pointed out that, as anticipated in Sec. I and discussed in detail in Sec. IV, these relaxation pulses are not simple exponen-

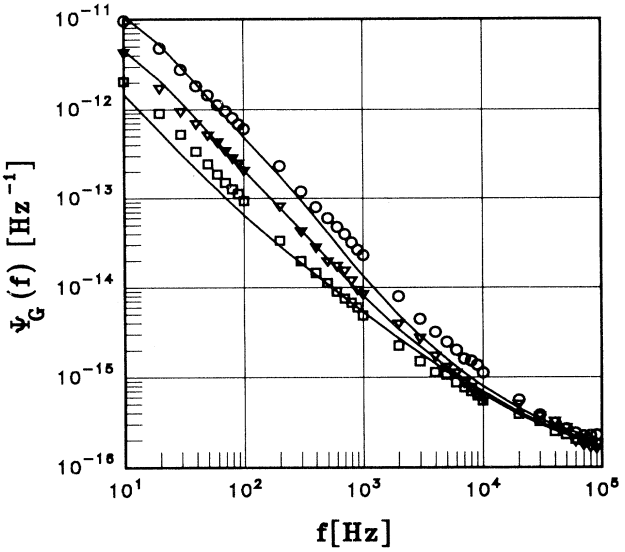

FIG. 2. Power spectra of the relative conductance fluctuation noise $\psi_G(f)$ taken at $\lambda=490$ nm and at 300 (circles), 250 (triangles), and 225 K (squares). The average electrical conductance ($G=2\times10^{-5}$ S) is the same for all spectra. Points are experimental, and correspond to local averages of the plotted curves over several runs. Continuous lines are theoretical from Eq. (3). Numerical values refer to $\psi_G(f)=4\pi\psi_G(\omega)$.

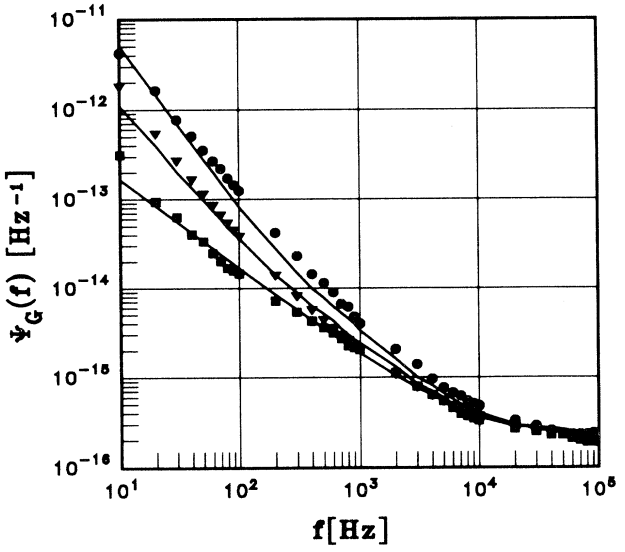

FIG. 3. Same as in Fig. 2 except that $\lambda=510$ nm, corresponding to a photon energy lower than the energy gap of CdS. The lower values of the noise spectral density at 10 Hz are related to the longer lifetime of the ionized deep donor centers with respect to that of the trapped holes created by light of wavelength shorter than λ_{gap} (see Fig. 4). At low temperature the strong increase of τ_d gives rise to a cutoff frequency of the photoinduced component that becomes much lower than 10 Hz, and the $1/f$ component of the intrinsic noise dominates the low-frequency range of the power spectrum.

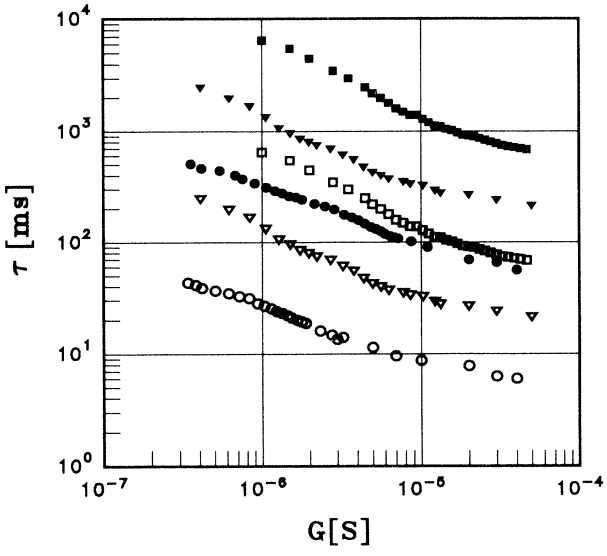

FIG. 4. Average decay time τ_d of the photocurrent at $\lambda=490$ (hollow symbols) and 510 nm (filled symbols) vs conductance G. The values of the temperature were 300 (circles), 250 (triangles), and 225 K (squares). The curves were obtained from a set of measurements of the type reported in Fig. 5, as described in the text. Estimated errors are approximately represented by the dots dimensions.

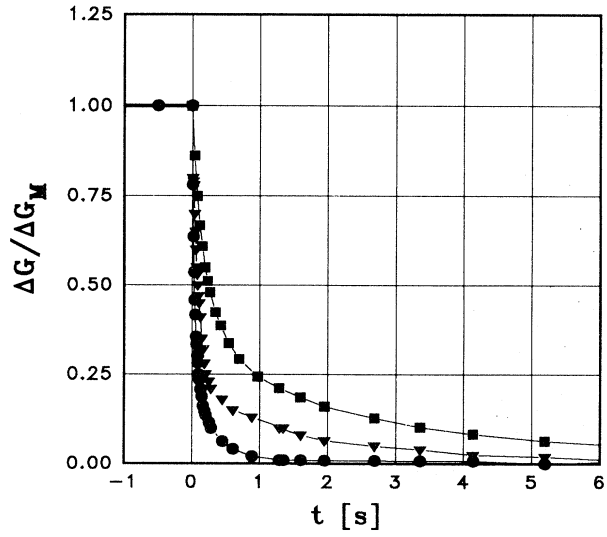

FIG. 5. Normalized phototransient decay curves at $\lambda=510$ nm and at 300 (circles), 250 (triangles), and 225 K (squares). The average conductance G is the same for the three curves, and corresponds to 2×10^{-5} S. Similar results, with a much shorter decay time, were obtained for $\lambda=490$ nm.

tials and can be interpreted as a superposition of exponential decays of time constants $\tau_d^{(j)}$. The relative weight $a^{(j)}$ of these exponentials determines the shape of the power spectrum of the photoconductance noise, while it does not affect the photoconductance, which depends only on the value of τ_d.

III. PHOTOCONDUCTION MODEL

In this section the barrier photoconduction model, used to develop the theory of current noise in devices based on photoconducting insulators as such CdS or CdSe,[4] is briefly sketched, and the main results are summarized.

Reference is made to a device constituted of a thin photoconducting film with symmetric Ohmic contacts, such as the one used to obtain the results presented in Sec. II. As shown in Ref. 4, even in the case of matching work functions between the metal electrodes and the photoconductor, a potential barrier is formed near the metal electrodes which prevents electrical conduction in the absence of light. In barrier photoconduction models, the electrical conduction is enhanced by the reduction under illumination of one or more barriers, according to different mechanisms. In Ref. 4, it is assumed that the barrier lowering is due to the presence of a positive trapped charge produced by light through the ionization of deep donor centers or the creation of trapped or little mobile holes, depending on the light wavelength. The long lifetime of this trapped charge justifies the long decay time of the photocurrent, as reported in Fig. 5, and also explains the abrupt change of this quantity observed in correspondence of λ_{gap}. Actually, in the case of CdS, for $\lambda < \lambda_{\text{gap}}$ the positive trapped charge is constituted mainly of trapped holes having a smaller lifetime than ionized donor centers. The behavior of conductance vs light intensity, which is superlinear at low intensity values but becomes linear at higher intensities, is also clearly explained by the fact that in this second case the barrier height is controlled by a feedback effect produced by the negative space charge of the injected electrons. This means that, at high light intensity, the number of electrons injected from the electrode into the photoconducting material during their average transit time becomes equal to the number of ionized centers or trapped holes created by light during their average lifetime τ_d.

As shown in the Sec. IV, the quantitative development allows a good check of the model by comparing theoretical and experimental curves obtained for different light wavelengths and temperatures. This photoconduction model also gives the correct amplitude and shape of the power spectrum of the conductance noise under different physical conditions.

The main results concerning the conductance and the conductance noise worked out in Ref. 4 are reported below. As already stated above, the final expression of the photoconductance has been obtained by considering that the barrier is crossed according to a thermally activated process and by calculating the height of the barrier in terms of the positive trapped charge and of the negative electronic space charge. The final implicit expression for the conductance G is

$$G = G_0 \exp\left\{ \frac{L_D e E_0}{kT} \left[n_d^* - \frac{Gd}{e\mu S} \right] \times \left[1 + \ln \frac{\phi_0}{L_D e E_0 \left[n_d^* - \frac{Gd}{e\mu S} \right]} \right] \right\}, \tag{1}$$

where

$$G_0 = \frac{2}{h^3} (2\pi m^* kT)^{3/2} \exp\left[-\frac{\phi_0}{kT} \right] e\mu \frac{S}{d} . \tag{2}$$

In Eq. (1), G_0 is the dark electrical conductance of the device, n_d^* is the density of the ionized donor centers or trapped holes produced by light, ϕ_0 is the dark barrier height, μ is the electron mobility, m^* is the electron effective mass, and S and d, respectively, are the cross-section area of the photoconducting film and the distance between the electrodes.

The quantity L_D is the effective Debye length, and E_0 the tangential component of the electric field in correspondence with the metal electrodes, created by a uniform charge density of one elementary positive charge per unit volume distributed within the photoconductor. The other symbols have the usual meaning.

As already stated in Sec. I, the fluctuation of the barrier height, related to the normal fluctuation of the number of ionized deep donor centers or trapped holes, is the origin of photoinduced noise component. Except in the case where the light intensity is very low, this component dominates the noise power spectrum in the low-frequency range. However, since the cutoff frequency of this component is roughly inversely proportional to τ_d, which, according to results of Fig. 4, increases rapidly when temperature decreases, this range is gradually shifted toward lower frequencies when the device is cooled. The photoinduced component has the advantage of being characterized by quantities that can be obtained directly from experiments. Some of these quantities are very sensitive to temperature, light wavelength, and light intensity. A comparison between experimental and theoretical results should thus allow a good check of the theory.

The general expression for the normalized photoconductance fluctuation spectrum has been worked out in Ref. 4 and is reported below:

$$\psi_G(\omega) = \frac{1}{G^2} \left[g \Delta g \tau_g \frac{\langle |S(\omega)|^2 \rangle}{\tau_g^2} n_d + 2(\Delta g)^2 \frac{|\langle S(\omega) \rangle|^2}{\tau_g^2} n_d \sum_j \frac{a^{(j)} \tau_d^{(j)}}{1 + \omega^2 \tau_d^{(j)2}} \right] . \tag{3}$$

The meaning of the symbols is the following: g is the contribution to the conductance G of the device of a single electron in the conduction band; Δg is the average increment of the conductance of the device related to the change of barrier height due to the excess ionization of a

single deep donor center (or due to a trapped hole) during its lifetime τ_d; τ_g is the average lifetime of an electron in the conduction band of the photoconductor, related to trapping processes in shallow centers, grain boundaries, and surface states; n_d is the average total number of the ionized donor centers or trapped holes in the illumination condition determining the conductance. It is related to the ionized donor or trapped hole density n_d^*, appearing in Eq. (1), by the relation $n_d = n_d^* \Omega$, where Ω is the photoconductor volume; and $a^{(j)}$ is the relative weight of the ionized centers of type j, whose lifetime is $\tau_d^{(j)}$, in the same illumination condition. By definition it is $\sum_j a^{(j)} = 1$. Finally the quantities $\langle |S(\omega)|^2 \rangle$ and $|\langle S(\omega) \rangle|^2$ respectively, represent the average of the square modulus and the square modulus of the average of the Fourier transform of a square conductance pulse of unitary amplitude and duration $\tau_g^{(i)}$. The distribution of the lifetimes $\tau_g^{(i)}$ of the electrons in the conduction band of the photoconducting material is discussed in Ref. 4, and is the origin of the generation-recombination (g-r) and $1/f$ noise components, whose power spectrum is given by the first term within square brackets in Eq. (3). This term represents an intrinsic noise generated by the trapping-detrapping processes which free electrons undergo in shallow centers while they cross the photoconducting material. The second term within square brackets represents the photoinduced noise component produced by the barrier fluctuation. As already stated above and extensively discussed in papers Refs. 4 and 5, it contains only quantities obtainable from experiments. Actually $|\langle S(\omega) \rangle|^2 / \tau_g^2$ is very nearly a constant, whose value is $1/2\pi$, and Δg is, by definition, the derivative of the conductance G with respect to n_d:

$$\Delta g = dG/dn_d \ . \tag{4}$$

n_d can be expressed in terms of the photon flux n_f:[4]

$$n_d = \eta_\lambda n_f \tau_d \ . \tag{5}$$

In the last equation η_λ is a coefficient representing the light quantum efficiency required to create the positive trapped charge for the considered wavelength, and τ_d is the average photocurrent relaxation time, defined as the area-to-height ratio of the relaxation pulse following a small change of light produced by a rectangular light signal added to the bias illumination.[8] As shown from the results reported in Fig. 4, τ_d is strongly dependent on temperature, light intensity, and wavelength. It determines the behavior of the photoconductance and its fluctuation under different physical conditions. The quantity η_λ cannot be directly measured on the device, but the whole set of measurements reported here is very well reproduced by the theory assuming a quite reasonable value of this quantity, which turns out to be independent of temperature and light intensity while also presenting an abrupt change, as expected, when λ crosses λ_{gap}.

A comparison between theoretical and experimental results is given in Sec. IV. All relevant quantities appearing in Eqs. (1) and (3) are obtained from the curves of G vs n_f and from the photoconductance relaxation, taken in different conditions of temperature, light intensity, and wavelength. The distribution of the $\tau_d^{(j)}$ could have been obtained by fitting these relaxation curves with a sum of exponentials, but the more reliable light modulation technique, described in Ref. 5, was used.

IV. DISCUSSION

To make a check of the photoconduction model, a comparison between the experimental results reported in Sec. II and the predictions of Eqs. (1) and (3) concerning photoconductance and photoconductance noise is reported in the following. The quantities $\tau_d^{(j)}$, n_d, and Δg appearing in these equations were obtained from the curves reported in Figs. 1 and 5, and from their definitions [Eqs. (4) and (5)].

Let us first consider the dependence of the photoconductance on temperature, and make a comparison with the predictions of Eq. (1). Since, according to the model, the conductance of the device depends on the barrier height, which is determined by number of trapped holes or ionized deep donor centers, it is more convenient to express G in terms of n_d instead of n_f. To convert n_f to n_d, Eq. (5) and the curves of τ_d vs G reported in Fig. 4 have been used. Figures 6 and 7 give the behavior of g vs n_d for different values of the temperature. The quantum efficiency coefficient η_λ in Eq. (5) has been taken as a best-fit parameter independent of temperature. It turns out to be 0.35 for λ just below λ_{gap}, where light absorption becomes complete. From Eq. (5) and the data reported in Figs. 1 and 4, the value of $\eta_{510} = 0.27\eta_{490}$ was

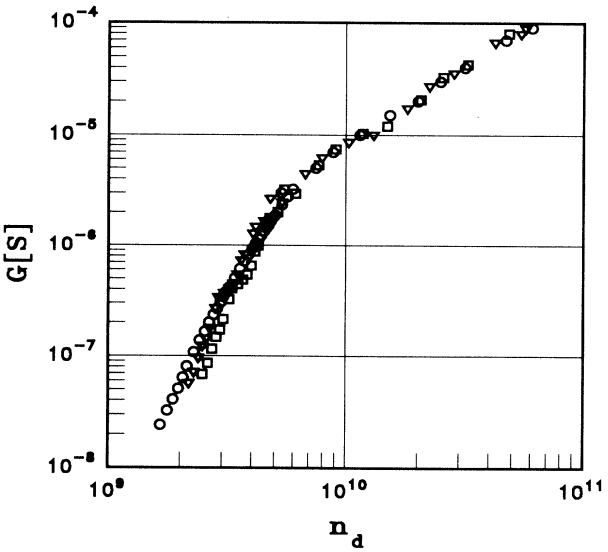

FIG. 6. Average conductance G at $\lambda = 490$ nm as a function of the total average number of ionized deep donor centers or trapped holes n_d at 300 (circles), 250 (triangles), and 225 K (squares). As expected from the model, the curves of G vs n_d are independent of the temperature. They have been obtained by using Eq. (5) and the data reported in Figs. 1 and 4 to evaluate n_d at different values of the conductance G. The value of η_λ at 490 nm has been taken as a best-fit constant parameter, independent of temperature and light intensity. Its value turns out to be 0.35.

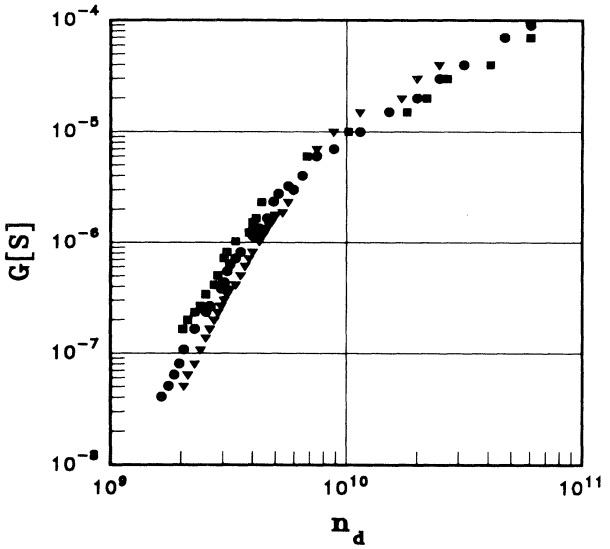

FIG. 7. Same as Fig. 6 but for $\lambda=510$ nm, corresponding to a photon energy lower than the energy gap. These data are coincident with those of Figs. 6 and 7, as predicted by the theory. The value of η_λ turns out to be lower than in the previous case ($\eta_{510}=0.27\times\eta_{490}=0.095$). The lower value is partly due to a much lower absorption coefficient of CdS at this λ value, which makes the film partially transparent to the light. However, the photoconductance at a constant photon flux is larger than at $\lambda=490$ nm, owing to a strong increase of τ_d (see Fig. 4).

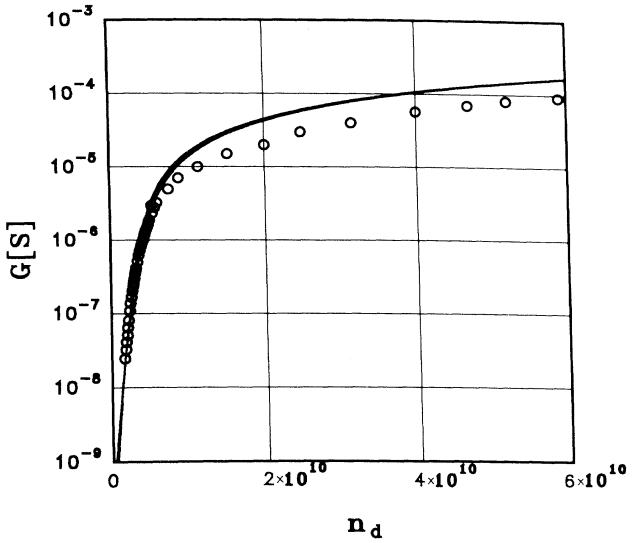

FIG. 8. Comparison between experimental and theoretical values of the photoconductance G vs n_d. As seen from the results of Fig. 6, when G is plotted vs n_d, all experimental points obtained at different wavelengths and temperatures fall on the same curve. Continuous lines are theoretical and correspond to the three values of the temperature given in Figs. 6 and 7. These curves, which are practically coincident, were obtained from Eq. (1) using the values of ϕ_0 reported in Table I. The other parameters appearing in this equation, which are independent of temperature, are given and discussed in Ref. 4. As stated in the text, the value of ϕ_0 influences only the initial slope of the curves and does not change their value above the knee, as better evidenced by the use of semilogarithmic scales. Circles correspond to the experimental data given in Fig. 6 at 300 K.

obtained.

As expected from the model, when G is plotted vs n_d, the curves corresponding to different values of temperature and wavelength overlap. This is due to the fact that the different values of the photoconductance obtained for the same value of the photon flux when the wavelength is changed are due to a different efficiency of the light in producing ionized donor centers or tapped holes and to the associated change of their lifetime. This last quantity is also strongly dependent on temperature, as the results of Fig. 4 show. These changes are automatically taken into account when n_d instead of n_f is considered, since n_d is proportional to the positive trapped charge, which determines the actual value of the potential barrier and thus the device conductance.

The fact that η_λ can be considered independent of temperature, so that n_d will depend only on the measurable quantities τ_d and n_f, shows very good agreement between theory and experiments when temperature is changed. A more stringent check of the theory is given in Fig. 8, where theoretical curves calculated from Eq. (1) are reported. The values of the quantities independent of temperature appearing in this equation are the same given and discussed in Ref. 5. The quantity G_0, needed to evaluate the barrier height, was obtained by measuring the dark conductance of the device after keeping it in the dark for several hours. In photoconducting insulators, dark conductivity decreases slowly with time after exposition to light, and this effect is enhanced at low temperatures, where eventually the phenomenon of persistent conductivity takes place.[9–11] This may be explained with the presence of trapping centers characterized by a very long lifetime increasing when temperature decreases, as τ_d does. Equation (2) was then used to evaluate the barrier height ϕ_0, which turns out to be slightly dependent on temperature (see Table I). In the same table the values of ϕ_0 used to fit the photoconductance vs light intensity curves at the different temperatures are reported.

The temperature dependence of ϕ_0, as well as the fact that the best-fit values of this quantity in the presence of light are slightly different from the ones obtained in dark conditions, may be attributed to the presence of a variable amount of persistently trapped charge which lowers the barrier and increases with light and with the lowering of the temperature. In any case it must be stressed that the value of ϕ_0 influences only the initial slope of the photoconductance vs light intensity curve. Actually, as already discussed above, at higher light intensity the photoconduction process is dominated by a balancing mechanism between the positive charge produced by light and the negative charge created by the injected electrons, and becomes insensitive to the value of ϕ_0. In this case there are no adjustable parameters, except for what concerns the electron mobility, which has been taken to be equal to the value given in the literature for pure CdS ($\mu=3\times10^{-2}$ $m^2V^{-1}s^{-1}$). The lower values of the ex-

TABLE I. Values of the potential barrier ϕ_0 appearing in Eqs. (1) and (2). The values of ϕ_0 in the first column have been obtained from experimental values of the dark conductance G_0 by means of Eq. (2). The values of ϕ_0 in the second column correspond to the best-fit parameters of Eq. (3) to the data reported in Fig. 6. The slight variations of this quantity with temperature and with respect to its best-fit values under illumination can be attributed to the presence of deep-lying centers having very long lifetimes and creating a short of "frozen" positive charge as in the case of the persistent photoconductivity.

T (K)	ϕ_0 (eV)	ϕ_0 (eV)
300	0.61±0.01	0.54
250	0.53±0.01	0.46
225	0.51±0.01	0.42

perimental points with respect to the theoretical curves, obtained at the highest values of the photoconductance (see Fig. 8), might be attributed to the fact that the value of the electron mobility of the device was lower than the one used in the calculations.

To compare the theoretical results given by Eq. (3) with the experimental noise power spectra, the values of Δg vs G, given in Fig. 9, were calculated from the derivative of the curves reported in Fig. 6. Even in this case it is interesting to note that, according to the theory, for high conductance values Δg should tend to g, independently of temperature and light wavelength.[4] In the case of the photoconducting device used in the present set of measurements, one obtains

$$g = e\mu/d^2 \cong 5\times 10^{-15}\ \text{S}\ , \tag{6}$$

where the value $d=1$ mm and the value of the electron mobility given above have been used. This value of g is in good agreement with that obtained from the curves of Fig. 9. However, if, as stated above, the value of the electron mobility is in fact lower than the one assumed in Eq. (6), to obtain agreement with the results of Fig. 9 a lower value of d should also be assumed. Since in Eq. (6) g is inversely proportional to d^2, small adjustments of this quantity could account for larger variations of μ. A precise measurement of d was, on the other hand, prevented by the fact that the photoconducting film was enclosed in a vacuum glass container. Furthermore, some indium diffusion within CdS in correspondence of the electrodes could have taken place.

Let us first consider the photoinduced component of the conductance noise, which is the one most influenced by temperature. The intrinsic noise component, which, according to the theory, takes into account only the fluctuation generated during the charge transport within the photoconducting material, may be considered independent of temperature when G is kept constant. For the g-r component this is confirmed by experiments, which show that, at high frequencies, where this component dominates, the noise power spectrum becomes independent of temperature, as the results of Figs. 2 and 3 show.

The photoinduced noise spectrum $\psi_G^{\rm ph}(\omega)$ is given by

$$\psi_G^{\rm ph}(\omega)=\frac{1}{\pi}\left[\frac{\Delta g}{G}\right]^2 n_d \sum_j \frac{a^{(j)}\tau_d^{(j)}}{1+\omega^2\tau_d^{(j)2}}\ , \tag{7}$$

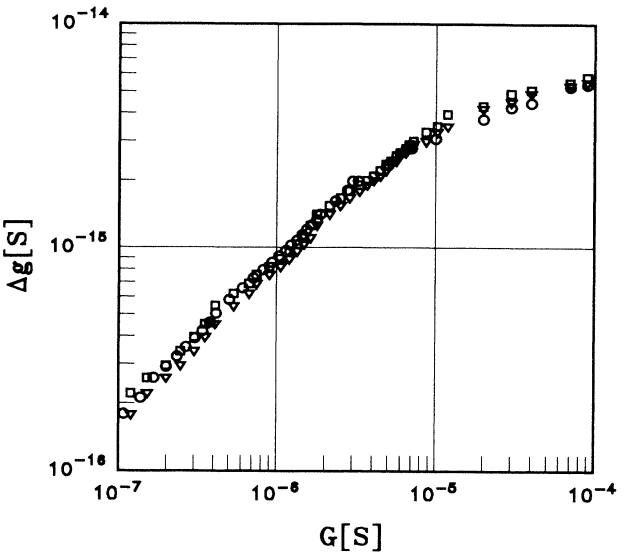

FIG. 9. Average conductance derivative with respect to n_d, as a function of the average conductance G for $\lambda=490$ nm and at 300 (circles), 250 (triangles), and 225 K (squares). This quantity has been obtained directly from the data of Fig. 6. Practically coincident results are obtained from the data of Fig. 7. According to the model, the quantity Δg tends to g for high light intensities independently of temperature and light wavelength. For CdS, since the electron mobility μ is practically independent of temperature in the considered range of variation (Ref. 7), g turns out to be a constant equal to 5×10^{-15} S [see Eq. (6)].

with $\sum_j a^{(j)}=1$. If, as a first approximation, the photocurrent relaxation is assumed to be characterized by a single exponential decay with time constant given by τ_d, Eq. (7) can be rewritten

$$\psi_G^{\rm ph}(\omega)=\frac{1}{\pi}\left[\frac{\Delta g}{G}\right]^2 n_d \frac{\tau_d}{1+\omega^2\tau_d^2}\ . \tag{8}$$

When the temperature T is changed and the conductance G is kept constant by adjusting the light intensity, the quantity mostly affected by the temperature variation in Eq. (8) is τ_d. Actually, according to the results previously shown in Figs. 6 and 9, both Δg and n_d can be considered independent of T. The strong variation of τ_d with temperature is shown in Figs. 4 and 5. According to Eq. (8), in the range of frequencies where $\omega^2\tau_d^2 \gg 1$, the power spectral density of the photoinduced component behaves as $1/\tau_d(T)$. Since τ_d generally increases when T decreases, a reduction of the photocurrent noise is expected when temperature is lowered. Such a behavior is qualitatively in agreement with the experiments, which show that at low temperature the photoinduced noise component becomes negligible with respect to the $1/f$ component in the explored range of frequencies. Quantitative results are reported in Figs. 2 and 3, which show the spectra calculated from Eq. (3) by taking into account the distribution of the time constants $\tau_d^{(j)}$ instead of the average value τ_d. The quantities $\tau_d^{(j)}$, together with their

TABLE II. Values of lifetimes $\tau_d^{(j)}$ and their relative weight $a^{(j)}$, corresponding to the noise spectra reported in Figs. 2 and 3. These values have been obtained according to the technique described in Ref. 5.

	$T=300$ K		$T=250$ K		$T=225$ K	
$\lambda=510$ nm	$\tau_d^{(1)}=400$ ms	$a^{(1)}=0.777$	$\tau_d^{(1)}=1000$ ms	$a^{(1)}=0.626$	$\tau_d^{(1)}=5280$ ms	$a^{(1)}=0.703$
	$\tau_d^{(2)}=40$ ms	$a^{(2)}=0.216$	$\tau_d^{(2)}=400$ ms	$a^{(2)}=0.283$	$\tau_d^{(2)}=1130$ ms	$a^{(2)}=0.218$
	$\tau_d^{(3)}=4$ ms	$a^{(3)}=0.007$	$\tau_d^{(3)}=100$ ms	$a^{(3)}=0.092$	$\tau_d^{(3)}=204$ ms	$a^{(3)}=0.079$
$\lambda=490$ nm	$\tau_d^{(1)}=100$ ms	$a^{(1)}=0.396$	$\tau_d^{(1)}=300$ ms	$a^{(1)}=0.547$	$\tau_d^{(1)}=830$ ms	$a^{(1)}=0.853$
	$\tau_d^{(2)}=10$ ms	$a^{(2)}=0.504$	$\tau_d^{(2)}=50$ ms	$a^{(2)}=0.174$	$\tau_d^{(2)}=81$ ms	$a^{(2)}=0.103$
	$\tau_d^{(3)}=1$ ms	$a^{(3)}=0.1$	$\tau_d^{(3)}=8$ ms	$a^{(3)}=0.279$	$\tau_d^{(3)}=14$ ms	$a^{(3)}=0.044$

relative weights $a^{(j)}$, were obtained by the modulation technique described in Ref. 5. Their values for different temperatures are reported in Table II.

The intrinsic noise components for the two values of λ are the same as reported in Refs. 4 and 5. Actually, as already stated, this component is assumed to be independent of temperature.

V. CONCLUSIONS

In this paper it has been shown that an extended set of experimental results concerning photoconductance and photoconductance noise in a CdS-based photoconducting device, taken at different values of temperature and light wavelength, are in good agreement with the prediction of a theory developed on the basis of a barrier-type photoconduction model.

The model neatly accounts for the abrupt change that the device responsivity and noise undergo when the light wavelength is changed in correspondence with λ_{gap}. Also, the relative changes shown by these quantities when the temperature is varied are accounted for without the introduction of free parameters.

It should be noted that even in the rather limited range of variation of the temperature reported in the present paper (from 300 to 225 K), several quantities related to the photoconduction process present a change up to an order of magnitude, so that a check of the theory seems quite convincing. A further reduction of the temperature gives rise to the onset of the well-known phenomenon of the persistent photoconductivity.[9–11] A possible explanation of the origin of this effect assumes the existence of deep-lying centers with large lattice relaxation times at low temperature.[12,13] In the ambit of the present model, the delayed recombination of these centers gives rise to a long-lasting lowering of the potential barrier at the metal-photoconductor interface. As already discussed in Sec. IV, the apparent decrease of ϕ_0 with temperature in the presence of light (see Table II) might also be related to the existence of these centers.

[1]R. H. Bube, *Photoconductivity of Solids* (Wiley, New York, 1964).
[2]J. C. Slater, Phys. Rev. **103**, 1631 (1956).
[3]R. L. Petritz, Phys. Rev. **104**, 1508 (1956).
[4]A. Carbone and P. Mazzetti, Phys. Rev. B **49**, 7592 (1994).
[5]A. Carbone and P. Mazzetti, Phys. Rev. B **49**, 7603 (1994).
[6]K. M. Van Vliet and J. Blok, Physica **22**, 231 (1956).
[7]R. H. Bube, *Photoelectronic Properties of Semiconductors* (Cambridge University Press, Cambridge, 1992).
[8]In Ref. 5, the values of τ_d at room temperature were taken by superimposing a short light flash on the main light flux, instead of a rectangular waveform light signal. This led to smaller values of this quantity, as already discussed in Sec. II, and forced us to assume an excessively large quantum efficiency ($\eta_\lambda=0.95$ at $\lambda=490$ nm) to fit the experimental results concerning photoconductance vs light intensity. The fitting of the noise power spectra was not influenced by this technical error, since their absolute values depend, as for photoconductance, on the product $\tau_d\eta_\lambda$, while their shape depends on the time constant distribution $\tau_d^{(j)}$ which was obtained with the light modulation technique described in the same paper.
[9]A. Rose, *Concepts in Photoconductivity and Allied Problems* (Wiley, New York, 1963).
[10]M. I. Korsunskii, *Anomalous Photoconductivity* (Wiley, New York, 1973).
[11]M. K. Sheinkman and A. Ya. Shik, Fiz. Tekh. Poluprovodn. **10**, 209 (1976) [Sov. Phys. Semicond. **10**, 128 (1976)].
[12]D. V. Lang and R. A. Logan, Phys. Rev. Lett. **39**, 635 (1977).
[13]D. V. Lang, R. A. Logan, and M. Jaros, Phys. Rev. B **19**, 1015 (1979).